FULL PAPER

Light-Gating Titania/Alumina Heterogeneous Nanochannels with Regulatable Ion Rectification Characteristic

Qianqian Zhang, Ziying Hu, Zhaoyue Liu, Jin Zhai,* and Lei Jiang*

Bioinspired artificial nanochannels exhibiting ion transport properties similar to biological ion channels have been attracting some attention for biosensors, separation technologies, and nanofluidic diodes. Herein, an easily available artificial heterogeneous nanochannel shows both ion gating and ion rectification characteristics when irradiated by ultraviolet light. The fabrication of heterogeneous nanochannels includes the coating of an anatase TiO_2 porous layer on an alumina porous supporter, followed by a chemical modification with octadecyltrimethoxysilane (OTS) molecules. The irreversible decomposition of OTS molecules by TiO_2 photocatalysis under ultraviolet light results in a change of surface wettability and an asymmetric distribution of surface negative charges simultaneously, which contributes to the ion gating and ion rectification. The asymmetric distribution of negative charges in the TiO_2 porous layer can be controlled by the irradiation time of ultraviolet light, which regulates the ion rectification characteristic.

1. Introduction

The predictably responsive transport of ions through biological ion channels is a fundamental process for life activities.[1] Ion gating that ion channels can open and close for ion transport under external stimuli is an important characteristic of biological ion channels.[1c,2] Inspired by biological ion channels, creation of artificial nanochannels with ion gating characteristic has attracted recently significant interest.[3] Generally, ion gating characteristic is realized by modifying the surface of artificial nanochannels with specific stimuli-responsive moieties, such as voltage-, pH-, temperature-, ion- or light-responsive molecules.[4–8] In particular, light-gating artificial nanochannels are of significant interest because of their ability to achieve remote and noninvasive in situ control.[9] Light-induced wettability conversion has been used to realize ion gating characteristic.[10,11] In a hydrophobic state, water solution is difficult to enter the nanochannels, which results in a closed state. In a hydrophilic state, water solution permeates the nanochannels easily, which results in an open state. Realizing such a wettability conversion by light stimulus leads to a dramatic change in ion current, which achieves light-gating artificial nanochannels.

Ion rectification that ions flow in a preferential direction is another important characteristic of biological ion channels.[1,3b] By rationally designing an asymmetric charge distribution, light-gating artificial nanochannels can be endowed with ion rectification characteristics.[8e–h] When light-responsive molecules are modified onto the surface of conic nanochannels, the nanochannels demonstrate light-gating ion transport and ion rectification characteristics simultaneously.[8e–i] However, because the asymmetric charge distribution is induced by the inherent asymmetric geometry,[12] the extent of ion rectification characteristic in these light-gating artificial nanochannels is difficult to be regulated.[8e–i] In addition, the fabrication of conic nanochannels always includes a complex procedure.[13] Therefore, creating easily available light-gating artificial nanochannels and regulating their ion rectification characteristics still remain challenges.

In this work, we demonstrate easily available light-gating TiO_2/Al_2O_3 heterogeneous nanochannels with regulatable ion rectification characteristic. The fabrication process is shown in **Scheme 1**. An anatase TiO_2 porous layer is coated on an Al_2O_3 porous supporter, which is subsequently modified with octadecyltrimethoxysilane (OTS) molecules.[14] TiO_2 photocatalysis induced by ultraviolet (UV) light is used to decompose OTS molecules irreversibly,[15] which results in a conversion of surface wettability[14,15a,16] and an asymmetric distribution of surface negative charges simultaneously, contributing to the ion gating and ion rectification characteristics. The asymmetric distribution of negative charges in TiO_2 porous layer is controlled by the irradiation time of UV light, not by the inherent channel geometry, the ion rectification characteristic therefore can be regulated.

2. Results and Discussion

Because of the robust mechanical property, light inertness and high-density pore distribution, anodic alumina was used as a

Dr. Q. Zhang, Z. Hu, Prof. Z. Liu, Prof. J. Zhai, Prof. L. Jiang
Key Laboratory of Bio-Inspired Smart Interfacial Science and Technology of Ministry of Education
School of Chemistry and Environment
Beihang University, Beijing, 100191, China
E-mail: liuzy@buaa.edu.cn; zhaijin@buaa.edu.cn

DOI: 10.1002/adfm.201301426

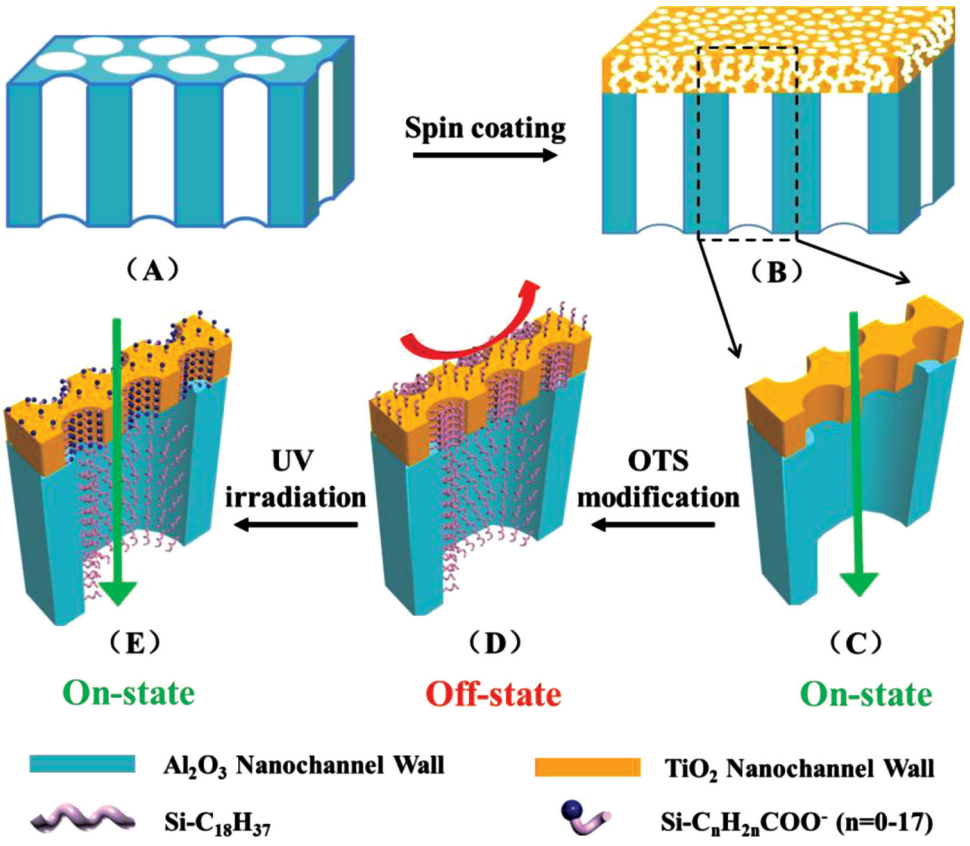

Scheme 1. Flow chart for the fabrication of octadecyltrimethoxysilane (OTS)-modified TiO_2/Al_2O_3 heterogeneous nanochannels. (A) Al_2O_3 porous supporter. (B) TiO_2 porous layer was deposited by spin-coating on an Al_2O_3 supporter. (C) Conceptual scheme of magnified TiO_2/Al_2O_3 heterogeneous nanochannels (On-state). (D) OTS molecules were modified on the heterogeneous nanochannels, which made the two sides of heterogeneous nanochannels become hydrophobic (Off-state). (E) After UV irradiation, TiO_2 side of heterogeneous nanochannels became hydrophilic gradually (On-state). Simultaneously, carboxylic groups were introduced in the nanopores of TiO_2 layer. The nanochannels in TiO_2 porous layer were conceptualized to be cylindrical shape.

supporter to fabricate TiO_2/Al_2O_3 heterogeneous nanochannels. As shown in **Figure 1**a, the pore average diameter of Al_2O_3 is determined to be ~216 nm with a distribution from 197 nm to 231 nm (Figure S1). The shape of Al_2O_3 nanochannels is cylindrical (Figure S2). After coating with a large-scale TiO_2 porous layer, the surface of Al_2O_3 supporter demonstrates almost no cracks and defects (Figure 1b). The cross-sectional image (Figure 1c) indicates that the heterogeneous nanochannels show a double-layer structure of TiO_2 porous film and Al_2O_3 porous supporter. The thickness of TiO_2 porous layer is ~227 nm. The immobilization of TiO_2 porous film on the surface of Al_2O_3 supporter is achieved by oxygen bridge bonds produced by the hydrolysis of Ti precursors with the surface hydroxyls of Al_2O_3.[17] Furthermore, the condensation of Ti precursors under heating forms a three-dimensional interconnected network structure of TiO_2, which avoids the collapse of TiO_2 porous film on the top of the Al_2O_3 nanopores. The diameter of nanopores embedded in TiO_2 porous layer is observed by TEM measurements to be ~3.8 nm with a distribution from 2.9 nm to 4.7 nm (Figure S3), which provides ions transport channels (Figure 1d, Figure S4 and Figure S5). It is necessary to mention that the geometric structure of TiO_2 porous layer may be considered to be symmetric because of the homogeneous mix of titanium precursor and F127 surfactant.

The crystallization of TiO_2 porous layer was characterized by wide-angle X-ray diffraction (WAXRD). As shown in **Figure 2**, when TiO_2 coating is dried at 80 °C, no resolved diffraction peaks are detected, indicating an amorphous phase (Figure 2a). After being annealed at 400 °C, the XRD pattern displays several strong and well-resolved diffraction peaks, which can be indexed to anatase phase (Figure 2b). Generally, anatase TiO_2 shows high photocatalytic activity because of their effective photogenerated electron-hole seperation.[18]

After OTS chemical modification, the two sides of heterogeneous nanochannels exhibit hydrophobicity (**Figure 3**). This is because the surface wettability is controlled by the hydrophobic terminal CH_3 groups of OTS molecules. The difference in the contact angles on Al_2O_3 side (~149.3°) and TiO_2 side (~136.1°) is ascribed to the different surface morphology and roughness. When UV light is irradiated on TiO_2 side, the water contact angle on TiO_2 side dramatically decreases, reaching a stable value of ~65.1° after 120 min irradiation. For Al_2O_3 side, water contact angle is not affected by UV irradiation obviously, keeping at ~137.9°.

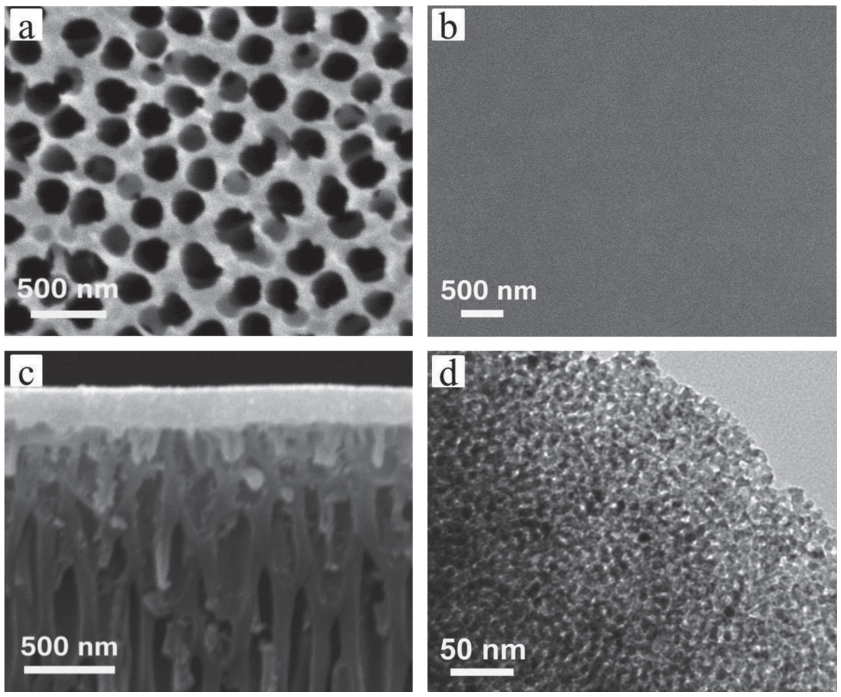

Figure 1. (a–c) Top-view and cross-sectional SEM images of TiO_2/Al_2O_3 heterogeneous nanochannels. (a) Al_2O_3 side, (b) TiO_2 side and (c) cross-section. (d) TEM image of unsupported TiO_2 porous film. The heterogeneous nanochannels show a double-layer structure of TiO_2 porous film and Al_2O_3 porous supporter. The mean pore diameter of Al_2O_3 nanochannels is ~216 nm and that of the TiO_2 nanopores is ~3.8 nm.

The significant change of contact angle on the TiO_2 side is ascribed to the strong photocatalytic properties of anatase TiO_2.[16] Under UV irradiation, photo-induced electron-hole separation occurs in anatase TiO_2.[19] The strong oxidation ability of photogenerated holes decomposes octadecyl chains ($Si\text{-}C_{18}H_{37}$) in OTS molecules, leaving carboxylic groups accompanying with the shortening of hydrocarbon chains ($Si\text{-}C_nH_{2n}COOH$, n = 0–17).[8i,20] There is no obvious change of water contact angle on Al_2O_3 side under long-term UV irradiation, which indicates that the UV-induced decomposition of OTS on Al_2O_3 side is negligible.

The ion transport properties of OTS-modified TiO_2/Al_2O_3 heterogeneous nanochannels after UV irradiation on TiO_2 side were characterized by measuring the current-voltage (I–V) curves. The electrolyte was 1 mM KCl aqueous solution. As comparison, we also measured the I–V curves of heterogeneous nanochannels without OTS modification after UV irradiation. The ion rectification ratio (f_R) was defined to be the ratio between the ion current values at –1.0 V (I_-) and +1.0 V (I_+), i. e. $f_R = |I_-|/|I_+|$. The UV-stimulated ion gating ratio (f_G) was defined to be the ratio between the ion current values at –1.0 V before (closed state, I_C) and after (open state, I_O) UV irradiation for different time, i.e., $f_G = |I_O|/|I_C|$.

As shown in **Figure 4**a, the unmodified heterogeneous nanochannels exhibit linear I–V curves and the magnitude of ion current remains constant after UV irradiation. The nanochannels do not demonstrate ion gating characteristic when irradiated by UV light. The ion rectification ratio (f_R) is ~1.0, which keeps unchanged with increasing time of UV irradiation. After modified with OTS molecules, the ion current of heterogeneous nanochannels is reduced significantly because of the surface hydrophobicity. The nanochannels remain as a closed state (Figure S6 and Figure S7). When UV light is irradiated on TiO_2 side in situ, the magnitude of ion current

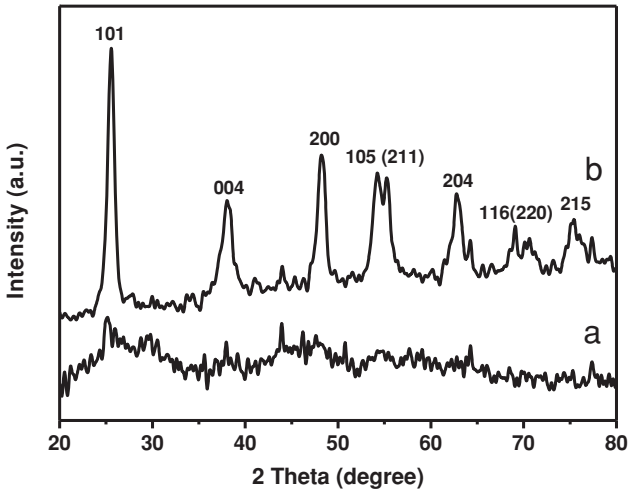

Figure 2. WAXRD patterns of TiO_2 porous film on Al_2O_3 supporter after (a) dried at 80 °C and (b) calcined at 400 °C. The XRD pattern of the sample after calcined at 400 °C displays well-resolved diffraction peaks of anatase phase, while the drying at 80 °C does not induce anatase crystallization.

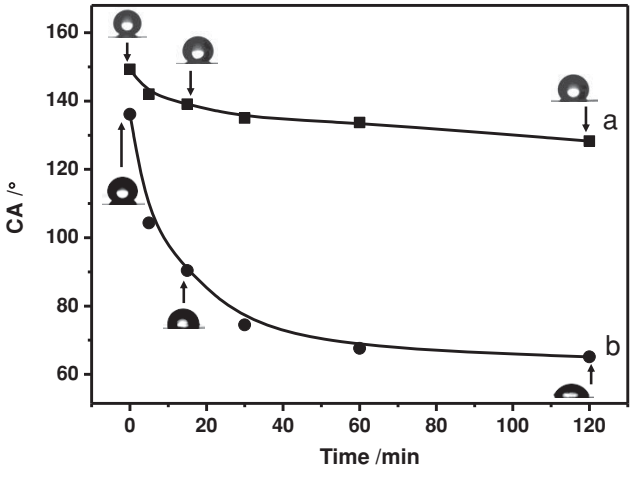

Figure 3. The evolution of water contact angles (CA) of OTS-modified TiO_2/Al_2O_3 heterogeneous nanochannels with the irradiation time of UV light on (a) Al_2O_3 side; (b) TiO_2 side. Under UV irradiation, water CA of the Al_2O_3 side stays nearly unchanged, while the water CA of the TiO_2 side decreases with the increasing of UV irradiation time then reaches a stable value.

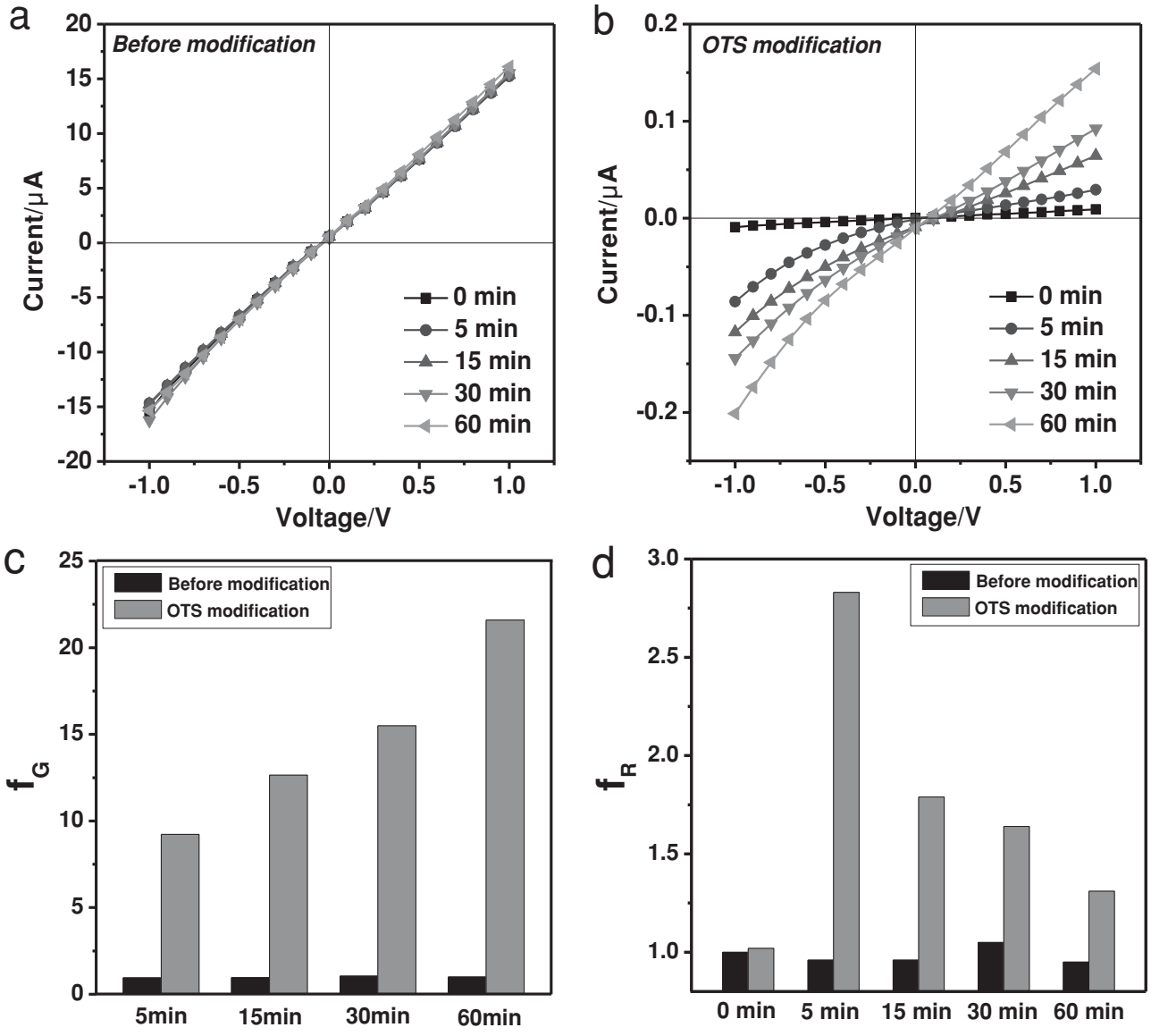

Figure 4. I–V properties of TiO_2/Al_2O_3 heterogeneous nanochannels (a) before and (b) after OTS modification when UV irradiation on TiO_2 side for different time. (c) The UV-stimulated ion gating ratio (f_G) of TiO_2/Al_2O_3 heterogeneous nanochannels at –1.0 V voltage before and after OTS modification. (d) Ion rectification ratio (f_R) of TiO_2/Al_2O_3 heterogeneous nanochannels before and after OTS modification. The UV light was irradiated on TiO_2 side in situ for different time. The unmodified heterogeneous nanochannels exhibit linear I–V curves and the magnitude of ion current remains constant after UV irradiation. After OTS modification, heterogeneous nanochannels show UV light-stimulated ion gating and tunable ion rectification properties. The electrolyte is fixed to be 1 mM KCl solution.

through OTS-modified TiO_2/Al_2O_3 heterogeneous nanochannels increases with the UV irradiation time varying from 0 min to 60 min (Figure 4b), which implies that the nanochannels are opened by the UV light. When the UV irradiation time is 60 min (the water contact angle is stable as shown in Figure 3), the ion gating ratio (f_G) at –1.0 V reaches ~21.6 (Figure 4c). More interestingly, after UV irradiation, the I–V curves of OTS-modified heterogeneous nanochannels are asymmetric (Figure 4b). As shown in Figure 4d, the f_R is about 1.0 before UV irradiation. The f_R dramatically increases to be ~2.9 after UV irradiation for 5 min. When increasing the time of UV irradiation, the f_R declines and finally reaches a stable value of ~1.3. It should be noted that no light-induced ion gating and ion rectification characteristics were detected in OTS-modified Al_2O_3 nanochannels (Figure S8).

The UV-stimulated ion gating and ion rectification characteristics of OTS-modified heterogeneous nanochannels can be ascribed to the conversion of surface wettability and the simultaneous introduction of surface negative charges in TiO_2 porous layer by the irreversible photocatalytic decomposition of OTS molecules.[14–16,20] The heterogeneous nanochannels in the KCl electrolyte can be considered as two series resistors of TiO_2 porous layer and Al_2O_3 supporter, which determine the magnitude of ion current. After OTS

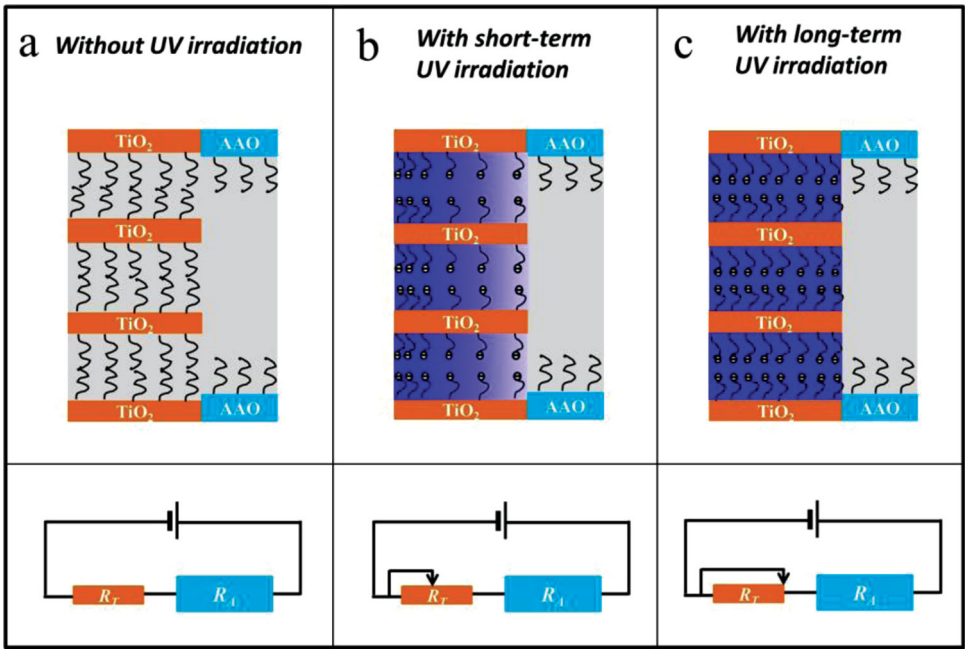

Scheme 2. Upper part: schematic illustration of charge distribution in TiO_2 porous layer of OTS-modified TiO_2/Al_2O_3 heterogeneous nanochannels after UV irradiation on TiO_2 side for different time. A dark blue color represents a high density of negative charges. The electrolyte is KCl aqueous solution. (a) Without UV irradiation. (b) With short-term UV irradiation. (c) With long-term UV irradiation. Lower part: Corresponding schematic drawing of the equivalent circuit of heterogeneous nanochannels (R_T: resistance of TiO_2 layer; R_A: resistance of Al_2O_3 layer). The nanochannels in TiO_2 porous layer are conceptualized to be cylindrical shape.

modification, the walls and surfaces of nanochannels are hydrophobic,[15a] which leads to a small magnitude of the ion current (**Scheme 2**a). Therefore, the heterogeneous nanochannel is in the closed state in darkness. With increasing the time of UV irradiation, the photocatalytic decomposition of OTS on the surface of TiO_2 porous layer converts the surface wettability of TiO_2 layer from hydrophobicity to hydrophilicity, which decreases the resistance of TiO_2 layer and increases the ion current (Scheme 2b). Therefore, the heterogeneous nanochannels are in an open state (Figure 4b). After UV irradiation for 60 min, TiO_2 layer is in a stable hydrophilic state (Scheme 2c), and the hydrophobic Al_2O_3 supporter alone restricts the ion transport.

Except for the surface wettability conversion, the photocatalytic decomposition of OTS molecules is considered to introduce hydrophilic carboxylic groups (–COOH) accompanying with the shortening of hydrocarbon chains.[20] In neutral KCl electrolyte, the carboxylic groups are ionized to yield negative charge ($–COO^-$) on the interior surface of TiO_2 nanopores because the pH of electrolyte is higher than its isoelectric point (pH ~ 3).[8i,21] The strong optical absorption of TiO_2 for UV light leads to a gradient distribution of carboxylic groups across TiO_2 layer. The density of carboxylic groups on the outside of TiO_2 layer (which accepts the light first) is larger than that on the inner side. In KCl electrolyte, the gradient distribution of carboxylic groups results in an asymmetric distribution of surface charges across TiO_2 porous layer, which is analogous to the asymmetric charge distribution induced by the asymmetric geometry (Scheme 2b).[12] The Debye length $1/\kappa$ formed in 1 mM KCl electrolyte is calculated to be ~9.8 nm, which is larger than the average pore radius of TiO_2 nanopores (~1.9 nm). Therefore, the TiO_2 layer demonstrates cations (K^+) selectivity, which rectifies the ion current.[22] When extending the time of UV irradiation, the UV-induced asymmetric distribution of negative charges in TiO_2 layer disappears gradually, which therefore decreases the ion rectification ratio (Scheme 2c). It is noteworthy to mention that the mean pore radius of Al_2O_3 supporter (~108 nm) is much larger than the Debye length in 1 mM KCl electrolyte. Furthermore, no negative charges are introduced onto the surface of nanopores in Al_2O_3 supporter after UV irradiation. Therefore, Al_2O_3 supporter with cylindrical channels has no effect on the ion rectification characteristic of heterogeneous nanochannels.

In order to validate that the ion rectification characteristic was induced by the surface carboxylic groups, we examined the effect of pH value on the I–V behaviors of OTS-modified heterogeneous nanochannels after UV irradiation for 5 min. As shown in **Figure 5**a, when the pH value of electrolyte is increased from 6.7 to 8.3, the f_R does not demonstrate significant change (~3.0). However, when the pH value is reduced to be 2.6, the f_R decreases to be 1.4 dramatically. Considering the isoelectric point of a surface with carboxylic groups is pH ~ 3,[21] under a pH close to isoelectric point, no excess negative charges distribute on the surface of TiO_2 nanopores, which leads to an almost linear I–V behavior. Our results confirm that the carboxylic groups produced by the photocatalytic decomposition of OTS contribute to the ion rectification.

We investigated the dependence of I–V behaviors of OTS-modified heterogeneous nanochannels after UV irradiation

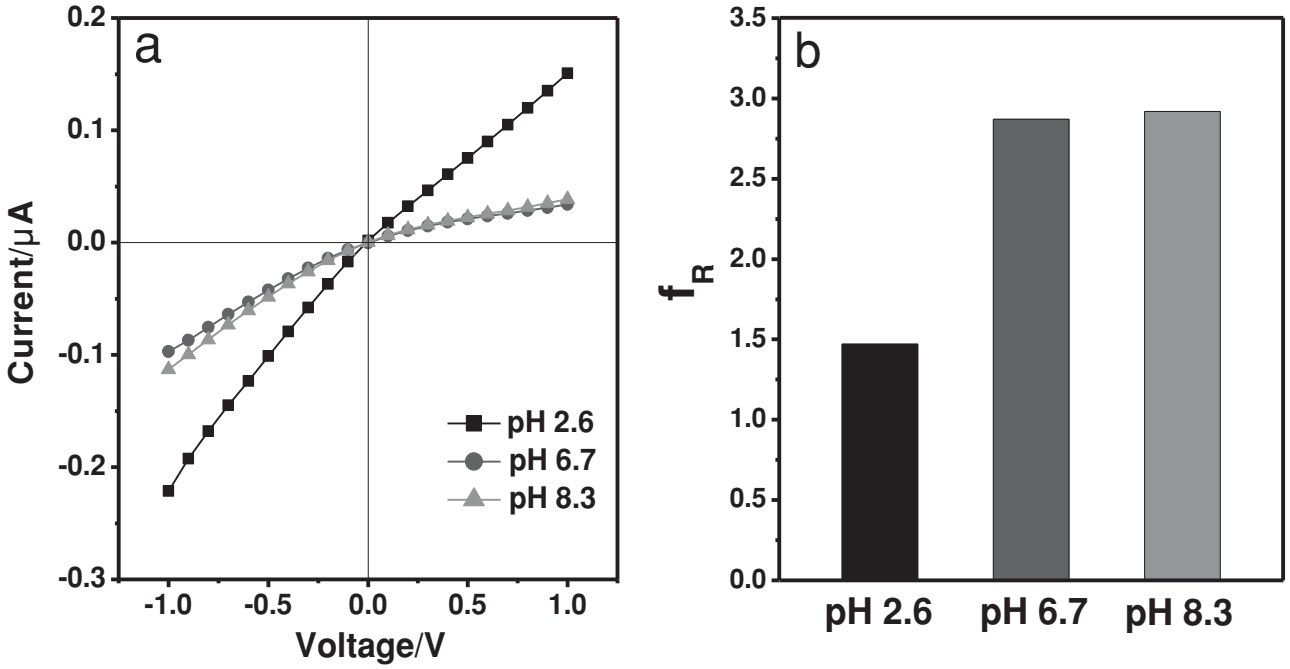

Figure 5. (a) I–V properties of OTS-modified TiO_2/Al_2O_3 heterogeneous nanochannels after UV irradiation on TiO_2 side for 5 min under different pH value in 1 mM KCl electrolyte. (b) The calculated ion rectification ratio (f_R). When the pH of electrolyte is 2.6 that close to isoelectric point of a surface with carboxylic groups, I–V behavior is almost linear and the f_R is ~1.4. The I–V curve becomes asymmetric and f_R increases when pH changes from 2.6 to 8.3.

on TiO_2 side for 5 min on the concentration of KCl electrolyte. As shown in **Figure 6**, the ion rectification ratio (f_R) is sensitive to the electrolyte concentration. When the electrolyte concentration is 0.01 mM, the nanochannels exhibit a remarkable ion rectification characteristic with an f_R of ~11.6. Subsequently, the f_R decreases when increasing concentration of KCl electrolyte. For 100 mM KCl electrolyte, the rectification ratio is ~1.1. The Debye length $1/\kappa$ in KCl electrolyte decreases with the increase of the electrolyte concentration.[23] When the concentration of KCl electrolyte is 100 mM, the calculated $1/\kappa$ is ~1.0 nm, which is smaller than the radius of TiO_2 nanopores (~1.9 nm). Therefore, TiO_2 layer does not demonstrate cations selectivity, which makes heterogeneous nanochannels exhibit no obvious ion rectification characteristic (Figure S9).

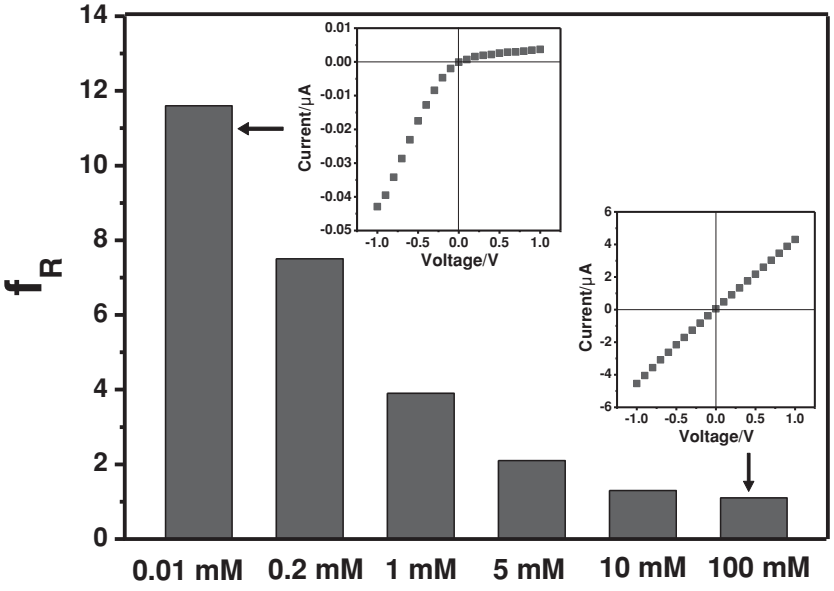

Figure 6. Ion rectification ratio (f_R) of OTS-modified TiO_2/Al_2O_3 heterogeneous nanochannels after UV irradiation on TiO_2 side for 5 min in KCl electrolyte with different concentrations. Inset: Examples of I–V curves of heterogeneous nanochannels under 0.01 mM and 100 mM KCl electrolyte. The f_R decreases with the increasing of the KCl electrolyte concentration. The voltage scanning range is fixed to be from –1.0 V to +1.0 V.

3. Conclusions

In conclusion, we have described OTS-modified TiO_2/Al_2O_3 heterogeneous nanochannels that exhibit light-tuned ion gating and ion rectification characteristics. When irradiated by the UV light, the UV-active photocatalysis of TiO_2 contributes to the change of surface wettability as well as the asymmetric distribution of surface negative charges, which realize the ion gating and ion rectification simultaneously. The gating property and rectification ratio of heterogeneous nanochannels can be regulated by the irradiation time of UV light. We anticipate that the heterogeneous nanochannels could readily be applied in some fields, such as sensors, seperation technologies, and micro/nanofluidic devices.

4. Experimental Section

Fabrication of Heterogeneous Nanochannels: In a synthesis process, 0.2 g of surfactant Pluronic F127 ($EO_{106}PO_{70}EO_{106}$, Aldrich) was dissolved in 4 ml absolute ethanol (Beijing Chemical Factory). Separately, 0.8 g of concentrated HCl (36 wt%, Beijing Chemical Factory) was added dropwise to 1.1 g titanium (IV) isopropoxide (TIPO, Acros) solution under vigorous stirring. The above two solutions were mixed with stirring for 3 h at ambient temperature. Then, the obtained homogeneous solution was poured into Petri dish, and aged at 10–20 °C and 60–80% relative humidity for 8–10 h without stirring. Uniform and transparent TiO_2 films were produced by spin-coating of the aged solution on one side of Al_2O_3 (AAO, Whatman) supporter at a constant spinning rate of 3000 rpm for 30 s. The films were heated at 80 °C in air for 12 h to evaporate the solvent completely. The as-prepared thin films were subsequently annealed at 400 °C for 3 h to remove F127 surfactant and induce TiO_2 crystallization[24].

Octadecyltrimethoxysilane (OTS, Aldrich) modification was achieved by chemical vapor deposition (CVD) method.[14] TiO_2/Al_2O_3 heterogeneous nanochannels were placed in a Teflon-lined stainless autoclave with OTS (60 μg), which was heated to 130 °C and kept at this temperature for 3 h. After modification, the two sides of nanochannels became hydrophobic, which was proved by the measurements of contact angle.

Subsequently, TiO_2 side of OTS-modified heterogeneous nanochannels was irradiated with ultraviolet (UV) light with a wavelength of 365 nm from a super-high pressure mercury lamp (CHF-XM500, Beijing Trusttech Co. Ltd, China). The UV irradiation time was 5 min, 15 min, 30 min, and 60 min. The irradiance of UV light was determined to be 2 mW cm^{-2} measured with a power meter (UV-A, Photoelectric Instrument Factory of Beijing Normal University).

Ion Current Measurements: The ion transport characteristics of OTS-modified heterogeneous nanochannels before and after UV irradiation for different time were characterized by measuring the ion current. The nanochannels were mounted between two chambers of the electrochemical cell with a quartz window (Scheme S1). TiO_2 side was irradiated by UV light in situ through a quartz window during the whole measurement. Potassium chloride (Beijing Chemical Factory) aqueous solution with different concentrations was chosen as electrolyte. Ion current was measured with a Keithley 6487 picoammeter (Keithley Instruments, Cleveland, OH). Ag/AgCl electrodes were used to apply a transmembrane voltage across the nanochannels because of their high sensitivity and good stability. The Al_2O_3 side of nanochannels was determined to be the positive potential. The transmembrane voltage varied from –1 V to +1 V. The testing temperature was the room temperature.

Characterization: The morphologies of heterogeneous nanochannels were characterized using a FEI Quanta FEG 250 environmental scanning electron microscope (SEM) and a JEOL-2100 transmission electron microscope (TEM). X-ray diffraction (XRD) patterns were recorded with a Shimadzu XRD-6000 X-ray diffractometer using Cu Kα radiation (40 kV, 40 mA) in the 2θ range of 20–80°. Water contact angles (CA) were measured using an OCA40 contact-angle system (DataPhyscics, Germany). Deionized water droplets (~5 μL) were dropped onto the surfaces. The test was carried out at ambient temperature and ca. 30% humidity.

Supporting Information

Supporting Information is available from the Wiley Online Library or from the author.

Acknowledgements

This work was supported by the National Basic Research Program of China (2011CB935704), National Natural Science Foundation of China (21003008, 21073009), Beijing Natural Science Foundation (2133066), Fundamental Research Funds for the Central Universities and Scientific Research Foundation for the Returned Overseas Chinese Scholars, State Education Ministry of China. We thanks Dr. Kefeng Wang for the drawing.

Received: April 26, 2013
Revised: June 14, 2013
Published online: August 19, 2013

[1] a) B. Hille, *Ion Channels of Excitable Membranes*, Sinauer Associates, Sunderland, MA **2001**; b) Z. S. Siwy, S. Howorka, *Chem. Soc. Rev.* **2010**, *39*, 1115; c) X. Hou, W. Guo, L. Jiang, *Chem. Soc. Rev.* **2011**, *40*, 2385.

[2] a) C. R. Martin, Z. S. Siwy, *Science* **2007**, *317*, 331; b) I. Vlassiouk, T. R. Kozel, Z. S. Siwy, *J. Am. Chem. Soc.* **2009**, *131*, 8211.

[3] a) C. Dekker, *Nat. Nanotechnol.* **2007**, *2*, 209; b) X. Hou, L. Jiang, *ACS Nano* **2009**, *3*, 3339; c) B. Yameen, M. Ali, R. Neumann, W. Ensinger, W. Knoll, O. Azzaroni, *Nano Lett.* **2009**, *9*, 2788.

[4] a) C. C. Harrell, P. Kohli, Z. S. Siwy, C. R. Martin, *J. Am. Chem. Soc.* **2004**, *126*, 15646; b) T. James, Y. V. Kalinin, C. C. Chan, J. S. Randhawa, M. Gaevski, D. H. Gracias, *Nano Lett.* **2012**, *12*, 3437; c) B. Corry, M. Thomas, *J. Am. Chem. Soc.* **2012**, *134*, 1840.

[5] a) L. Wang, Y. L. Song, H. Ji, O. Y. Qi, Y. G. Wang, L. Jiang, *J. Am.Chem. Soc.* **2008**, *130*, 8345; b) B. Yameen, M. Ali, R. Neumann, W. Ensinger, W. Knoll, O. Azzaroni, *Nano Lett.* **2009**, *9*, 2788; c) B. Yameen, M. Ali, R. Neumann, W. Ensinger, W. Knoll, O. Azzaroni, *J. Am. Chem. Soc.* **2009**, *131*, 2070; d) M. Ali, P. Ramirez, S. Mafe, R. Neumann, W. Ensinger, *ACS Nano* **2009**, *3*, 603; e) X. Hou, Y. J. Liu, H. Dong, F. Yang, L. Li, L. Jiang, *Adv. Mater.* **2010**, *22*, 2440; f) B. Yameen, M. Ali, R. Neumann, W. Ensinger, W. Knoll, O. Azzaroni, *Chem. Commun.* **2010**, *46*, 1908.

[6] a) B. Yameen, M. Ali, R. Neumann, W. Ensinger, W. Knoll, O. Azzaroni, *Small* **2009**, *5*, 1287; b) W. Guo, H. W. Xia, F. Xia, X. Hou, L. X. Cao, L. Wang, J. M. Xue, G. Z. Zhang, Y. L. Song, D. B. Zhu, Y. G. Wang, L. Jiang, *ChemPhysChem* **2010**, *11*, 859; c) Y. H. Zhou, W. Guo, J. S. Cheng, Y. Liu, J. H. Li, L. Jiang, *Adv. Mater.* **2012**, *24*, 962.

[7] a) Z. S. Siwy, M. R. Powell, A. Petrov, E. Kalman, C. Trautmann, R. S. Eisenberg, *Nano Lett.* **2006**, *6*, 1729; b) M. R. Powell, M. Sullivan, I. Vlassiouk, D. Constantin, O. Sudre, C. C. Martens, R. S. Eisenberg, Z. S. Siwy, *Nat. Nanotechnol.* **2008**, *3*, 51; c) X. Hou, W. Guo, F. Xia, F. Q. Nie, H. Dong, Y. Tian, L. P. Wen, L. Wang, L. Cao, Y. Yang, J. Xue, Y. Song, Y. Wang, D. Liu, L. Jiang, *J. Am. Chem. Soc.* **2009**, *131*, 7800; d) Y. Tian, X. Hou, L. P. Wen, W. Guo, Y. L. Song, H. Z. Sun, Y. G. Wang, L. Jiang, D. B. Zhu, *Chem. Commun.* **2010**, *46*, 1682; e) M. Ali, S. Nasir, P. Ramirez, J. Cervera, S. Mafe, W. Ensinger, *ACS Nano* **2012**, *6*, 9247.

[8] a) N. G. Liu, D. R. Dunphy, P. Atanassov, S. D. Bunge, Z. Chen, G. P. López, T. J. Boyle, C. J. Brinker, *Nano Lett.* **2004**, *4*, 551; b) G. L. Wang, A. K. Bohaty, I. Zharov, H. S. White, *J. Am. Chem. Soc.* **2006**, *128*, 13553; c) L. P. Wen, X. Hou, Y. Tian, J. Zhai, L. Jiang, *Adv. Funct. Mater.* **2010**, *20*, 2636; d) L. P. Wen, X. Hou, Y. Tian, F. Q. Nie, Y. L. Song, J. Zhai, L. Jiang, *Adv. Mater.* **2010**, *22*, 1021; e) M. Ali, S. Nasir, P. Ramirez, I. Ahmed, Q. H. Nguyen, L. Fruk, S. Mafe, W. Ensinger, *Adv. Funct. Mater.* **2012**, *22*, 390; f) M. H. Zhang, X. Hou, J. T. Wang, Y. Tian, X. Fan, J. Zhai, L. Jiang, *Adv. Mater.* **2012**, *24*, 2424; g) L. P. Wen, Q. Liu, J. Ma, Y. Tian, C. H. Li, Z. S. Bo, L. Jiang, *Adv. Mater.* **2012**, *24*, 6193; h) L. P. Wen, J. Ma, Y. Tian, J. Zhai, L. Jiang, *Small* **2012**, *8*, 838; i) Z. Y. Hu, Q. Q. Zhang, J. Gao, Z. Y. Liu, J. Zhai, L. Jiang, *Langmuir* **2013**, *29*, 4806.

[9] a) M. Banghart, K. Borges, E. Isacoff, D. Trauner, R. H. Kramer, *Nat. Neurosci.* **2004**, *7*, 1381; b) A. Koçer, M. Walko, W. Meijberg,

B. Feringa, *Science* **2005**, *309*, 755; c) P. Gorostiza, E. Isacoff, *Mol. BioSyst.* **2007**, *3*, 686.

[10] I. Vlassiouk, C. D. Park, S. A. Vail, D. Gust, S. Smirnov, *Nano Lett.* **2006**, *6*, 1013.

[11] a) O. Beckstein, P. C. Biggin, M. S. P. Sansom, *J. Phys. Chem. B* **2001**, *105*, 12902; b) C. Brumaru, M. L. Geng, *Langmuir* **2010**, *26*, 19091; c) S. N. Smirnov, I. V. Vlassiouk, N. V. Lavrik, *ACS Nano* **2011**, *5*, 7453; d) M. Pevarnik, K. Healy, M. Davenport, J. Yen, Z. S. Siwy, *Analyst* **2012**, *137*, 2944; e) M. R. Powell, L. Cleary, M. Davenport, K. J. Shea, Z. S. Siwy, *Nat. Nanotechnol.* **2012**, *6*, 789.

[12] a) Z. S. Siwy, E. Heins, C. C. Harrell, P. Kohli, C. R. Martin, *J. Am. Chem. Soc.* **2004**, *126*, 10850; b) I. Vlassiouk, Z. S. Siwy, *Nano Lett.* **2007**, *7*, 552.

[13] Z. S. Siwy, P. Y. Apel, D. Baur, D. D. Dobrev, Y. E. Korchev, R. Neumann, R. Spohr, C. Trautmann, K.-O. Voss, *Surface Science* **2003**, *532–535*, 1061.

[14] L. L. Wang, X. T. Zhang, Y. Fu, B. Li, Y. C. Liu, *Langmuir* **2009**, *25*, 13619.

[15] a) J. P. Lee, H. K. Kim, C. R. Park, G. Park, H. T. Kwak, S. M. Koo, M. M. Sung, *J. Phys. Chem. B* **2003**, *107*, 8997; b) J. P. Lee, M. M. Sung, *J. Am. Chem. Soc.* **2004**, *126*, 28.

[16] a) A. Kanta, R. Sedev, J. Ralston, *Langmuir* **2005**, *21*, 5790; b) M. Järn, Q. Xu, M. Lindén, *Langmuir* **2010**, *26*, 11330.

[17] T. R. B. Foong, Y. Shen, X. Hu, A. Sellinger, *Adv. Funct. Mater.* **2010**, *20*, 1390.

[18] a) A. Fuhishima, T. Inoue, K. Honda, *J. Am. Chem. Soc.* **1979**, *101*, 5582; b) C. S. Turchi, D. F. Ollis, *J. Catal.* **1990**, *122*, 178; c) K. Ishibashi, Y. Nosaka, K. Hashimoto, A. Fujishima, *J. Phys. Chem. B* **1998**, *102*, 2117.

[19] a) A. Fuhishima, K. Honda, *Nature* **1972**, *238*, 37; b) Y. Ohko, T. Tatsuma, A. Fuhishima, *J. Phys. Chem. B* **2001**, *105*, 10016.

[20] T. Tatsuma, Sh. Tachibana, A. Fujishima, *J. Phys. Chem. B* **2001**, *105*, 6987.

[21] P. Apel, Y. E. Korchev, Z. S. Siwy, R. Spohr, M. Yoshida, *Nucl. Instr. Meth.in Phys. Res. B* **2001**, *184*, 337.

[22] a) Z. S. Siwy, A. Fuliński, *Phys. Rev. Lett.* **2002**, *89*, 198103; b) Z. S. Siwy, A. Fuliński, *Am. J. Phys.* **2004**, *72*, 567; c) Z. S. Siwy, *Adv. Funct. Mater.* **2006**, *16*, 735.

[23] K. Bohinc, V. Kralj-Iglič, A. Iglič, *Electrochim. Acta* **2001**, *46*, 3033.

[24] a) B. Tian, X. Liu, B. Tu, C. Yu, J. Fan, L. Wang, S. Xie, G. Stucky, D. Zhao, *Nat. Mater.* **2003**, *2*, 159; b) R. Zhang, B. Tu, D. Zhao, *Chem. Eur. J.* **2010**, *16*, 9977; c) J. Zhang, Y. Deng, D. Gu, S. Wang, L. She, R. Che, Z. Wang, B. Tu, S. Xie, D. Zhao, *Adv. Energy Mater.* **2011**, *1*, 241.